

1
2
3
4
5
6
7
8
9
10
11
12
13
14
15
16
17
18
19
20
21

Expanding the genetic toolkit of *Tribolium castaneum*

Johnathan C. Rylee¹, Dylan J. Siniard^{1,2}, Kaitlin Doucette¹, Gabriel E. Zentner^{1*}, Andrew C. Zelhof^{1*}

¹ Department of Biology, Indiana University, Bloomington, IN 47405

² Present address: Division of Asthma Research, Cincinnati Children’s Hospital Medical Center, Cincinnati, OH 45229

* Corresponding author

E-mail: gzentner@indiana.edu (GEZ)

E-mail: azelhof@indiana.edu (ACZ)

22 **Abstract**

23 The red flour beetle, *Tribolium castaneum*, is an important model insect and agricultural pest.
24 However, many standard genetic tools are lacking or underdeveloped in this system. Here, we
25 present a set of new reagents to augment existing *Tribolium* genetic tools. We demonstrate a
26 new GAL4 driver line that employs the promoter of a ribosomal protein gene to drive expression
27 of a UAS responder in the fat body. We also present a novel dual fluorescent reporter that
28 labels cell membranes and nuclei with different fluorophores for the analysis of cellular
29 morphology. This approach also demonstrates the functionality of the viral T2A peptide for
30 bicistronic gene expression in *Tribolium*. To facilitate classical genetic analysis, we created lines
31 with visible genetic markers by CRISPR-mediated disruption of the *yellow* and *ebony* body color
32 loci with a cassette carrying an attP site, enabling future ϕ C31-mediated integration. Together,
33 the reagents presented here will facilitate more robust genetic analysis in *Tribolium* and serve
34 as a blueprint for the further development of this powerful model's genetic toolkit.

35

36 **Introduction**

37 The red flour beetle (*Tribolium castaneum*), a pest of stored agricultural products, has emerged
38 as a promising system for biological research. It is a representative of the order Coleoptera,
39 which comprises approximately 40% of known insect species and 25% of all known animals [1].
40 While *Drosophila melanogaster* is by far the most popular insect model system, many aspects
41 of its development and physiology are not representative of insects in general, and so findings
42 in *Tribolium* may be more broadly applicable to insects in many cases. Furthermore, Coleoptera
43 includes significant agricultural pests such as the corn rootworm, Colorado potato beetle, and
44 Asian longhorn beetle, and so using *Tribolium* as an insect model may lead to advances in pest
45 control.

46 Advances in genetic tools have cemented the status of *Tribolium* as the second model
47 insect of choice behind *Drosophila*. Transgenic *Tribolium* may be obtained using various
48 transposons [2, 3] and more recently via CRISPR/Cas9-mediated genome editing [4]. Eye-
49 specific fluorescent markers have also been developed to aid identification of transgenics [2].
50 Transposition techniques have been used in for insertional mutagenesis, allowing the
51 identification of essential genes as well as enhancer traps [5]. Another valuable tool for
52 functional genomics, RNA interference (RNAi) via injection of eggs, larvae, or adults, has been
53 implemented in *Tribolium*, both in targeted studies [6-8] and in a large-scale screen of the
54 protein-coding genome [9]. Lastly, the GAL4/UAS system, a popular choice for spatiotemporally
55 controlled expression of a gene of interest in *Drosophila*, has been demonstrated to function in
56 *Tribolium* in the presence of a species-specific basal promoter [10].

57 Despite the proliferation of tools for genetic analysis and manipulation of *Tribolium*,
58 notable gaps remain. In the case of the GAL4/UAS system, only two driver lines are available,
59 one using a heat shock promoter [10] and the other making use of the odorant receptor co-
60 receptor (*Orco*) regulatory regions [11]. Furthermore, *Tribolium* strains with visible phenotypic
61 markers of known genetic location, which are staples of classical genetic analysis, are not
62 readily available. Here, we present a set of reagents to address these issues and enhance the
63 utility of *Tribolium* as a genetic model organism. We first present a GAL4 driver line that
64 employs a ribosomal gene promoter to direct expression in the fat body and can serve as an
65 second effective marker for transgenesis. In addition, we describe a GAL4-inducible cellular
66 reporter in which the nucleus and endomembrane system are labeled with different fluorescent
67 proteins, acting as a robust means by which to analyze cellular structure, particularly with
68 respect to neurons. Furthermore, both the GAL4 and UAS cloning vectors are designed to
69 accept any gene or genomic region of interest to generate new drivers and reporters. We also
70 address the lack of visible phenotypic markers in *Tribolium* by using CRISPR to disrupt two
71 genes involved in cuticle pigmentation via homologous recombination with cassettes containing

72 an attP site to facilitate future genomic insertion of DNA of interest using the ϕ C31 integrase.
73 The tools presented here represent a valuable resource for the *Tribolium* research community
74 and serve as a general template upon which further tools can be based.

75

76 **Materials and methods**

77 ***Tribolium* husbandry and strains**

78 All animals were raised at 28°C on a standard flour yeast mix. The following strains were
79 utilized: *v^W* and *m26* [3].

80 **Vectors**

81 All vectors will be made available through the *Drosophila* Genomics Resource Center at Indiana
82 University (<https://dgrc.bio.indiana.edu/Home>).

83 ***P119der***

84 119der, a derivative of pSLfa[UAS-Tc'Hsp-p-tGFP-SV40] (kindly provided by Dr. Gregor Bucher)
85 [10], was constructed by excision of tGFP with KpnI and NotI followed by replacement with the
86 sequence ACTAGTGAATTCAAAGTACCACTCGAGAGCGGCCGCG. This replacement
87 destroyed the KpnI site but preserved the unique NotI site and added a unique XhoI site.
88 (DGRC # XXXX)

89 ***P130der***

90 p130der, a derivative of pSLfa[Hsp-p-Gal4Delta-SV40_attp] (kindly provided by Dr. Gregor
91 Bucher) [10], was constructed by digestion with BamHI and addition of the sequence
92 GGATCCAGGTACCAGCGGCCGAGGATCC, containing unique KpnI and NotI sites. (DGRC
93 # XXXX)

94 ***pGZ286 (pBac-3xP3-EGFP-pTC006550-GAL4Δ)***

95 The basal *hsp68* promoter of PCR-linearized p130der was replaced with the *TC006550*
96 promoter amplified from blaAmp-Tc6550Pro-GFPZeo-Luciferase-HSP-Orange-pIZT (kindly
97 provided by Dr. Yoonseong Park) [12] with NEBuilder HiFi assembly (NEB). The resulting
98 p*TC006550-GAL4Δ-SV40* polyA coding sequence was then amplified and inserted into PCR-
99 linearized pBac[3xP3-EGFP] with NEBuilder HiFi assembly. (DGRC # XXXX)

100 ***pTC241 (pBac-3XP3-EGFP-UAS-nls-EGFP-T2A-mCherry)***

101 The nls-EGFP-T2A-mCherryCAAX insert was amplified from pSYC-102 (a gift from Seok-Yong
102 Choi, Addgene plasmid #74790) [13] as two fragments, and assembled into the NotI site of
103 p119der using NEBuilder HiFi assembly. UAS-nls-EGFP-T2A-mCherryCAAX was then excised
104 using flanking Ascl sites and ligated into pBac[3xP3-GFP]. (DGRC # XXXX)

105

106 **Immunofluorescence and imaging**

107 *Tribolium* larvae were dissected in PBS and tissue was fixed in 4% paraformaldehyde/PBS. The
108 tissue was washed 2X with PBT (PBS and 0.8% Triton-X 100) and incubated with DAPI (final
109 concentration of 0.1 µg/ml) for 10 minutes and then washed with PBS before mounting for
110 imaging (modified from [14]). Confocal images were captured on a Leica SP8 confocal utilizing
111 a Leica 63X oil immersion objective with a numerical aperture of 1.40. Light and fluorescent
112 whole animal images were collected on a LeicaMZ10F dissecting microscope. All pictures were
113 processed in Adobe Photoshop.

114

115 **CRISPR**

116 gRNAs were designed using CRISPRdirect [15] using the Tcas3 genome assembly for the
117 specificity check. Only high-quality gRNAs were selected. 20-mer protospacer sequences were
118 cloned into BsaI-digested pU6b-BsaI-gRNA [4] by NEBuilder HiFi-mediated ssDNA oligo

119 bridging as described (<https://www.neb.com/-/media/nebus/files/application-notes/construction->
120 [of-an-sgrna-cas9-expression-vector-via-single-stranded-dna-oligo-bridging-of-double-stranded-](https://www.neb.com/-/media/nebus/files/application-notes/construction-of-an-sgrna-cas9-expression-vector-via-single-stranded-dna-oligo-bridging-of-double-stranded-dna-fragments.pdf)
121 [dna-fragments.pdf](https://www.neb.com/-/media/nebus/files/application-notes/construction-of-an-sgrna-cas9-expression-vector-via-single-stranded-dna-oligo-bridging-of-double-stranded-dna-fragments.pdf)) using an ssDNA oligo consisting of the protospacer flanked by 25 bp regions
122 of vector homology. Protospacer sequences used were CCGGAAAATAATCTCCCAGT (*yellow*,
123 *TC000802*) and TTTCGTAAAAGTTTGAATCG (*ebony*, *TC0011976*) (DGRC #XXXX and
124 #XXXX). Homology donors consisting of an attP site and 3xP3-DsRed-SV40 polyA flanked by
125 loxP sites in the same orientation between 800 bp (*yellow*; left arm: ChLG2:7,663,877-
126 7,664,676, right arm: ChLG2:7,664,677-7,665,476) or 726/739 bp (*ebony*; left arm:
127 ChLG9:13,340,543-13,341,268, right arm: ChLG9:13,341,269-13,342,007) homology arms were
128 synthesized by IDT and delivered in pUCIDT-amp. Mixtures consisting of 400-500 ng/mL each
129 of Cas9 plasmid [4], sgRNA plasmid, and donor plasmid were injected into v^w embryos.

130

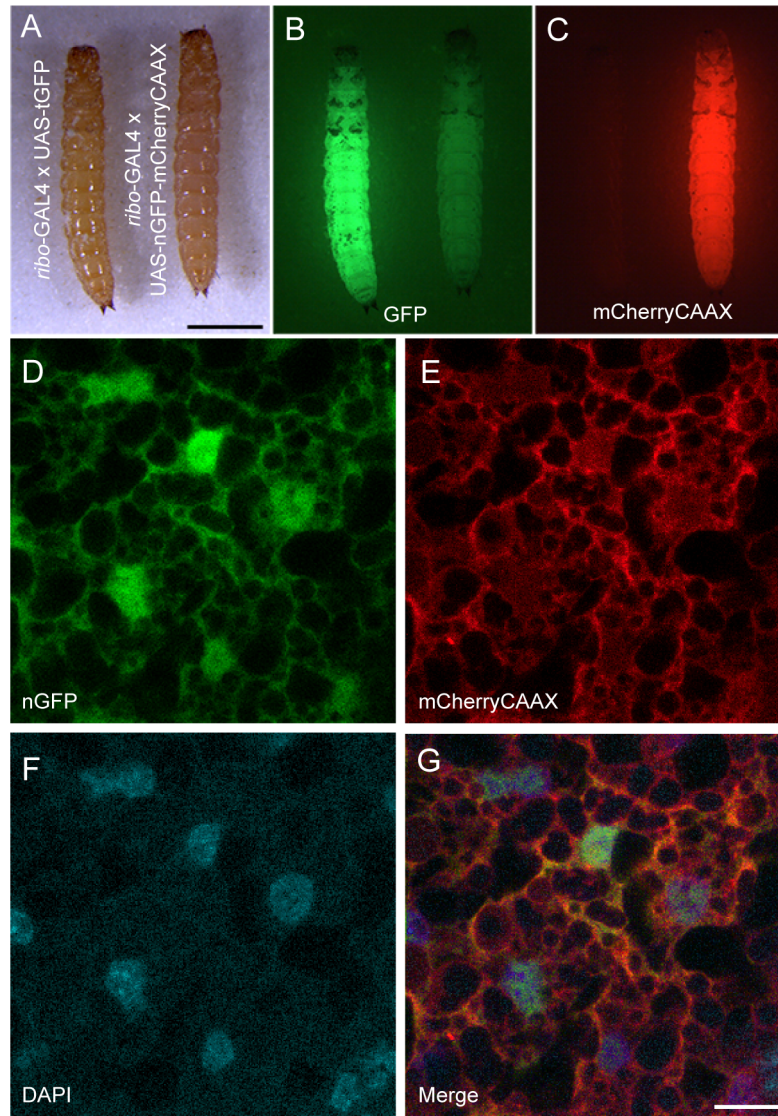
131 **Results**

132 **Construction and implementation of a *ribo-GAL4* driver**

133 Inducible expression of a transgene of interest is a key capability in any genetic model
134 organism. In *Drosophila*, the bipartite *Saccharomyces cerevisiae* GAL4/UAS (upstream
135 activating sequence) system, in which the GAL4 transcription factor binds to a 17-bp motif within
136 the UAS to drive transcriptional activation, is frequently used for spatiotemporally controlled
137 expression of a gene of interest [16]. In *Tribolium*, the GAL4-UAS system has been
138 demonstrated to be functional when the UAS is coupled with the *hsp68* basal promoter and
139 driven by heat shock-inducible GAL4 [10]. However, no ubiquitous GAL4 drivers have been
140 reported for *Tribolium*. Such drivers are useful when screening for an organismal or
141 developmental phenotype of overexpression or knockdown.

142 In an attempt to generate a ubiquitous and constitutive GAL4 driver line, we considered
143 a previous study in which the promoter of a ribosomal protein gene (*TC006550*) was used to
144 drive high-level expression in the *Tribolium* TcA cell line [12]. We thus replaced the heat shock
145 promoter of our p130der vector (see Materials and Methods), bearing the basal *hsp68* promoter
146 and GAL4 Δ , with the *TC006550* promoter. GAL4 Δ is a variant of GAL4 in which the N- and C-
147 termini, containing the DNA-binding and transcriptional activation domains, are directly fused
148 [17]. This variant of GAL4 has been shown to increase transactivation by ~2-fold in *Drosophila*
149 [18]. We then transferred the *TC006550* promoter and GAL4 Δ coding region to a piggyBac
150 vector containing 3xP3-EGFP, enabling selection of transgenics by fluorescence in
151 photoreceptors. This vector was injected into a *Tribolium* line lacking eye pigmentation
152 (*vermillion*^{white} (*v*^w)) with 3xP3-DsRed-marked piggyBac transposase integrated into the X
153 chromosome [3]. Resulting adults were outcrossed to *v*^w and progeny were assessed for GFP
154 expression in the retina. *TC006550-GAL4 Δ* transformants (hereafter referred to as *ribo-GAL4*)
155 were identified and the DsRed-marked transposase was removed through subsequent crosses
156 and two independent insertions were generated.

157 To assay the functionality of the *ribo-GAL4* driver line, we crossed it to a previously
158 described UAS-GFP responder line [10]. Larvae displayed strong whole-body fluorescence (Fig.
159 1A-C) and fluorescence is maintained throughout pupal development and into adulthood as
160 expected for a ubiquitous expression. However, further examination revealed fluorescence was
161 only detected in the putative fat body (Fig. 1D-G) and absent from other tissues (e.g. the gut,
162 muscle, and CNS). We speculate that the lack of ubiquitous GAL4 expression in the *ribo-GAL4*
163 line may reflect tissue-specific differences in ribosomal protein gene expression [19] and that,
164 given the apparent *in vivo* expression profile of *TC006550*, the TcA cell line may be derived
165 from fat cells.



166

167 **Figure 1. Characterization of GAL4 and UAS vectors.**

168 (A-C) *Tribolium* larvae expressing either GFP (left) or nls-EGFP-T2A-mCherryCAAX (right)
169 driven by *ribo*-GAL4. (A) White light illumination; (B) GFP illumination. The nls-EGFP signal is

170 not detectable as compared to cytoplasmic GFP. (C) mCherry illumination. Scale bar = 1 mm.

171 The mCherry illumination mimics the cytoplasmic GFP expression. (D-G) Images of fat cells
172 expressing nls-EGFP (D) and mCherryCAAX (E), counterstained with DAPI (F), and the merge

173 of the three labels (G). Each represents a single confocal section. Scale bar = 10 μ m.

174

175 **Construction and implementation of a reporter for cell** 176 **structure**

177 There are numerous reporters available for highlighting cell structure and function. Our goal was
178 to test whether these reporters could be simply swapped into a universal UAS cloning vector for
179 *Tribolium* with zero or minimal changes to the already existing sequence. We chose nls-EGFP-
180 T2A-mCherryCAAX [13] to test the utility of bicistronic fluorescent reporter expression for
181 studying cell morphology as well as the use of the viral T2A peptide in *Tribolium*. When
182 combined with our *ribo*-GAL4 line, mCherry expression could easily be detected in whole larvae,
183 mimicking the spatial and temporal pattern obtained with cytoplasmic GFP (Fig 1A-C). To
184 confirm the expression and localization of both the nuclear GFP and the endomembrane linked
185 mCherry we examined the subcellular localization of each in fat cells. Colocalization with DAPI
186 confirmed the subcellular localization of GFP in the nucleus with mCherryCAAX bound to
187 membranes (Fig 1D-G). These results indicate that existing fluorescent reporters can be easily
188 implemented in *Tribolium* using our UAS vector and that the T2A peptide can be used for
189 multicistronic gene expression in *Tribolium*.

190

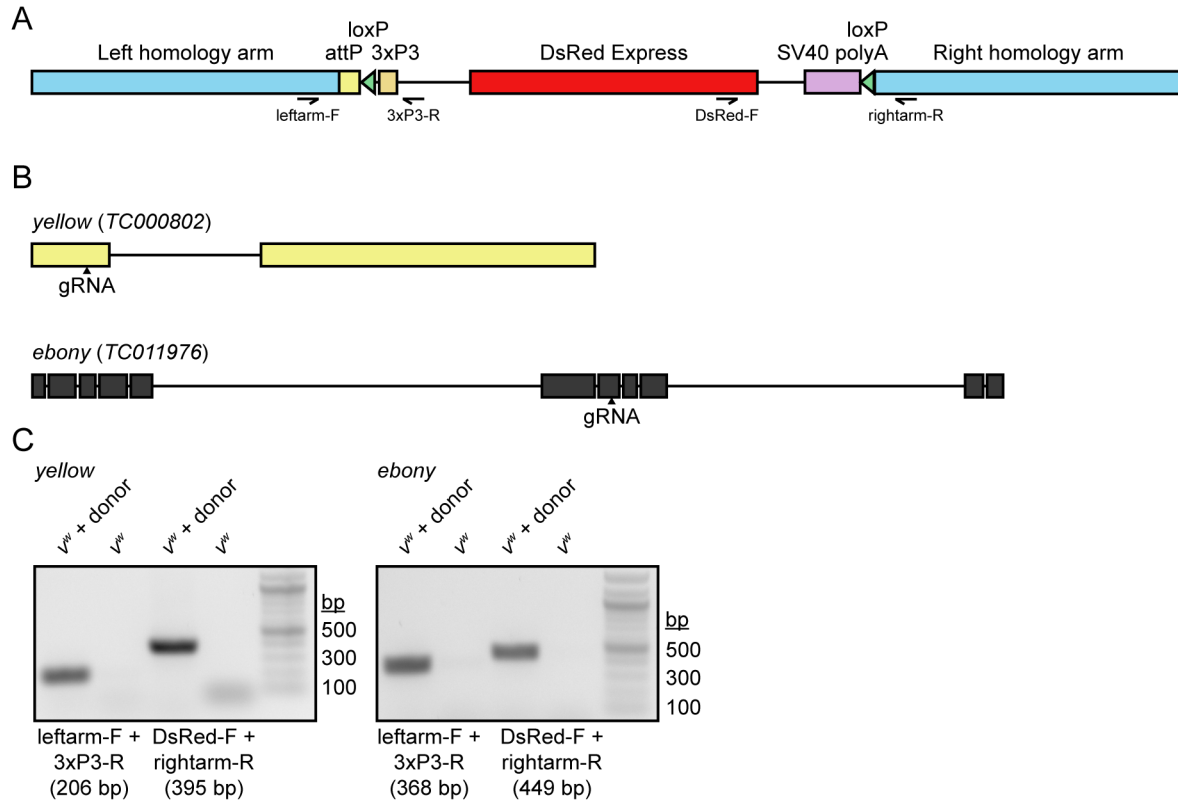
191 **CRISPR-based generation of lines with visible phenotypic** 192 **markers**

193 Defined phenotypic visible markers are essential for facilitating even basic tasks such as
194 establishment of stocks of genetically modified organisms or tracking of specific chromosomes
195 through multiple generations. While the scope of genetic reagents available in *Tribolium* has
196 markedly increased over the past few decades, there are notable limitations and gaps in
197 existing tools. For instance, the use of visible phenotypic markers for genetic mapping is quite
198 limited, especially compared to *Drosophila*, where variations in wings, bristles, eye and body

199 pigmentation, and body shape are available. Additionally, while dominant mutations giving rise
200 to visible phenotypes in *Tribolium* have been documented [20-22], they have not been mapped
201 to a tractable genetic interval in most cases and so cannot be used in such analyses.

202 In order to create a general strategy for the expansion of a pool of visible phenotypic
203 markers for *Tribolium*, we employed CRISPR based homologous recombination. We designed
204 gRNAs against the coding regions of the *yellow* (*TC000802*) and *ebony* (*TC011976*) genes, as
205 well as a disruption cassette with useful genetic features. In many insects, the disruption of
206 either *ebony* and *yellow* leads to viable and fertile animals that are easily identifiable from their
207 wild-type counterparts. With respect to our CRISPR procedure, we chose a homologous
208 recombination strategy that would permit detection of a disruption in either locus regardless of
209 whether a change in pigmentation resulted. For each targeting construct, we utilized 700-800
210 bp homology arms, and between them we enclosed an attP site to facilitate future ϕ C31
211 integrase-mediated insertion of DNA of interest at a defined location [23]. More importantly, we
212 included the DsRed Express fluorescent protein under the control of the eye-specific 3xP3
213 regulatory element to facilitate screening of CRISPR based recombinants; and two loxP sites in
214 the same orientation, enabling future Cre-mediated excision of 3xP3-DsRed from the genome
215 (Fig. 2A). The positioning of the loxP sites is such that they flank only the fluorescent marker
216 and so excision would leave the attP site intact, effectively recycling the DsRed marker for
217 further use.

218



219

220 **Figure 2. Construction and validation of the CRISPR gene disruption strategy.**

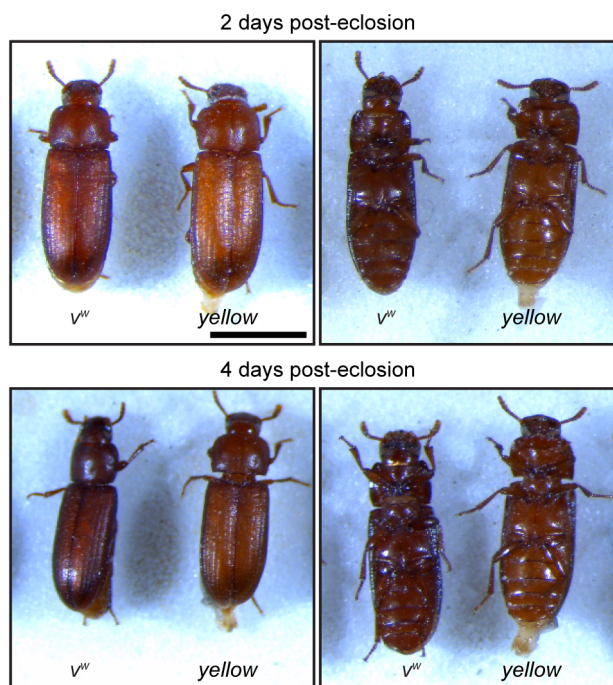
221 (A) Schematic representation of the gene disruption cassette used in this study. The positions
 222 and directionalities of primers used for genomic PCR validation are included in the schematic.
 223 (B) Positions of gRNAs used to disrupt the *yellow* and *ebony* loci. (C) Genomic PCR
 224 demonstrating the presence of each gene disruption cassette in the genome of transgenic but
 225 not parental beetles.

226

227 v^w embryos were injected with a mixture of Cas9 plasmids, gRNA expression plasmid,
 228 and repair template plasmids. Surviving adults were crossed to v^w and resulting progeny were
 229 screened upon eclosion for DsRed expression in the retina. For *yellow*, 308/356 injected larvae
 230 survived to adulthood and of these, two tested positive for germline transmission of the
 231 disrupted gene (0.65%). For *ebony*, 184/217 injected larvae survived to adulthood and of these,
 232 one tested positive for germline transmission of the disrupted gene (0.54%).

233 Characterization of *yellow*-edited adults revealed that cuticles of newly eclosed beetles
234 were noticeably lighter than those of their *v^w* counterparts, but their color darkened over time
235 until they were difficult to distinguish from the parental line (Fig 3). In contrast, adults with
236 homozygous disruption of *ebony* displayed substantially darker cuticular pigmentation than
237 parental *v^w* individuals (Fig. 4A-B) and DsRed fluorescence in their eyes (Fig. 4C). While *ebony*
238 CRISPR individuals were clearly phenotypically distinct from the parental line, their cuticle was
239 not as dark as individuals injected with *ebony* dsRNA ([http://ibeetle-base.uni-](http://ibeetle-base.uni-goettingen.de/details/TC011976)
240 [goettingen.de/details/TC011976](http://ibeetle-base.uni-goettingen.de/details/TC011976)). We speculate that this difference is due to the location of the
241 gRNA target site. It lies within the seventh exon of *ebony*, which falls after the sequences
242 encoding all but one predicted functional domain of the protein (Fig. 5). However, this gRNA
243 falls at the start of the last domain of the protein, and disruption of this domain likely explains the
244 hypomorphic phenotype observed.

245

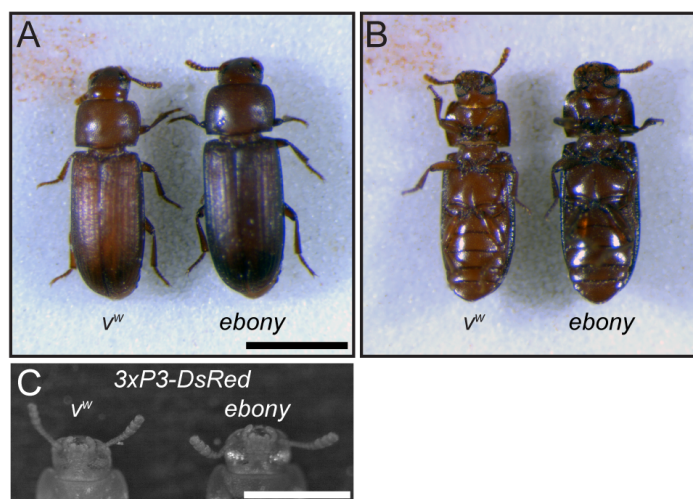


246

247 **Figure 3. Phenotypic characterization of *yellow* CRISPR beetles.**

248 Dorsal and ventral views of parental v^w and transgenic *yellow* CRISPR beetles at 2 and 4 days

249 post-eclosion. Scale bar = 1 mm.



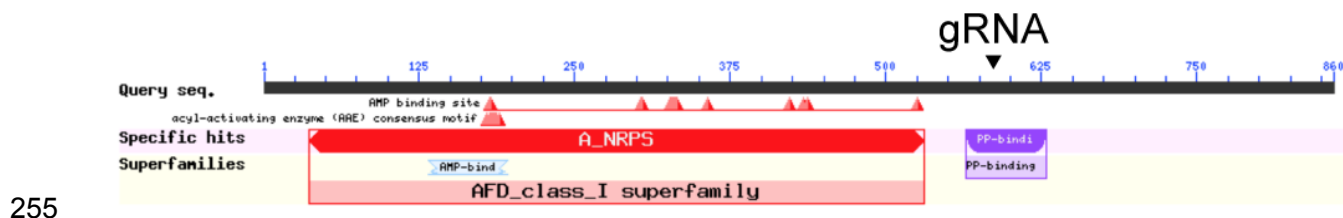
250

251 **Figure 4. Phenotypic characterization of *ebony* CRISPR beetles.**

252 (A) Dorsal and (B) ventral views of parental v^w and transgenic *ebony* CRISPR beetles. Scale bar

253 = 1 mm. (C) DsRed fluorescence microscopic image of the eyes of v^w and transgenic *ebony*

254 CRISPR beetles. Scale bar = 0.5 mm.



255
256 **Figure 5. NCBI conserved domain search results for the *ebony* protein.** The location of the
257 gRNA relative to the mature protein sequence is indicated.

258

259 Conclusions

260 Here, we present a series of reagents aimed at increasing the genetic tractability of
261 *Tribolium*. These are (1) a GAL4 driver plasmid and *Tribolium* line expressing GAL4 in fat cells;
262 (2) a UAS plasmid and UAS-inducible dual-nuclear/endomembrane fluorescence reporter for
263 analyzing cell structure; (3) a template gene disruption cassette for the generation of mutants
264 and insertion of attP sites; and (4) *Tribolium* lines carrying disruptions of two body color loci,
265 *yellow* and *ebony*.

266 We surmise that the failure of the *ribo*-GAL4 line to drive ubiquitous reporter expression
267 is attributable to its late pupal origin [24], reflecting cell type variability in *TC006550* expression.
268 Indeed, heterogeneity in ribosomal protein expression across cell types has been widely
269 reported [19, 25-27]. Other potential candidates for the establishment of a ubiquitous GAL4 line
270 include the *α-Tubulin1* promoter, which has been shown to drive ubiquitous GFP expression
271 throughout the *Tribolium* life cycle [28], and the *Polyubiquitin* promoter [29]. The p130der
272 plasmid permits efficient insertion of any potential genomic sequence for designing future GAL4
273 lines. Furthermore, our data demonstrates that any established reporter can be cloned into our
274 modified version of pSLfa[UAS-Tc'Hsp-p-tGFP-SV40] [10], p119der, for direct expression in
275 *Tribolium*. Future variations/deviations of both p130der and p119der will include an attB site for

276 direct insertion into known genomic positions as well as a fluorescent marker to enable rapid
277 screening of transgenics.

278 While we successfully disrupted the *yellow* and *ebony* loci via CRISPR, the visible
279 phenotypes associated with these editing events were unpredictable. In particular, disruption of
280 *yellow* resulted in a slow-tanning phenotype, with young adults displaying a visibly lighter cuticle
281 than the parental strain that then darkened until it was indistinguishable from that of non-edited
282 beetles. In the case of *ebony*, we were able to achieve a marked darkening of the cuticle using
283 our disruption strategy, but our mutation was potentially hypomorphic when compared to *ebony*
284 RNAi, which yielded a darker black-body phenotype. In order to maximise the visible
285 phenotypes obtainable with CRISPR disruption of an eye or body color locus, we therefore
286 recommend pre-screening of candidate visible marker genes with RNAi prior to initiating
287 genome editing. Several candidates for body eye and body color genes have been assessed by
288 RNAi in the literature [30-33] and may serve as suitable targets for our CRISPR disruption
289 approach. Moreover, our data demonstrate that the inclusion of an independent marker for
290 CRISPR-based modifications is invaluable in recovering transformants and thus can mitigate
291 the uncertainty associated with the targeting of other potential candidate loci for visible markers.

292

293

294 **Acknowledgments**

295 We thank Drs. G. Bucher, S. Brown, and M. Lorenzen for *Tribolium* reagents. We thank Dr. J.
296 Powers and the Indiana University Light Microscopy Imaging Center for assistance with image
297 generation. We thank Dr. M. J. Wade for helpful discussions throughout the course of this work.
298 This work was supported by Indiana University startup funds to G.E.Z. and the NSF (IOS-
299 1353267) to A.C.Z.

300

301

Primer	Sequence (5' → 3')	Application
pTC006550-F	GATCGATATCGGCGCGCCAACAGC	Amplification of the <i>TC006550</i> promoter from blaAmp-Tc6550Pro-GFPZeo-Luciferase-HSP-Orange-pLZT
pTC006550-R	CTCTAGTACCAACCTTACGTTAGAA TTGAGTTACGAG	
p130der-F	ACGTAAGGTTGGTACTAGAGGTACA CGTCTCCC	Linearization of p130der for insertion of the <i>TC006550</i> promoter
p130der-R	TTGGCGCGCCGATATCGATCGCGC GCAGA	
pTC006550-GAL4-SV40-F	CATAGGCCACGGCGCGCCAACA	Amplification of the <i>ribo</i> -GAL4 coding sequence from p130der
pTC006550-GAL4-SV40-R	CGGAGTGGACAGATACATTGATGA GTTTGGACAAACCAC	
pBac-F	CAATGTATCTGTCCACTCCGCCTTT AGTTTGATTATAATACA	Linearization of pBac[3xP3-EGFP] for insertion of the <i>ribo</i> -GAL4 coding sequence
pBac-R	TTGGCGCGCCGTGGCCTATGGCAT TATTGTACGGA	
nls-EGFP-F	ACTAGTGAATTCAAAGTACCACTCG AGAGCATGGCTCCAAAGAAAGAAG CGTAAGGTAAAT	Amplification of nls-EGFP from pSYC-102
nls-EGFP-R	CCTTAAGCTTGTACAGCTCGTCCAT GCCGA	
T2A-mCherry-CAAX-F	TCGGCATGGACGAGCTGTACAAGC TTAAGG	Amplification of T2A-mCherry-CAAX from pSYC-102
T2A-mCherry-CAAX-R	GTGGTATGGCTGATTATGATCTAGA GTCGCTCAGGAGAGCACACTTG CAGCTCATGCA	

302

303 **S1 Table. DNA oligonucleotides used in this work.**

304 References

- 305 1. Hunt T, Bergsten J, Levkanicova Z, Papadopoulou A, John OS, Wild R, et al. A
306 Comprehensive Phylogeny of Beetles Reveals the Evolutionary Origins of a Superradiation.
307 Science. 2007;318(5858):1913-6. doi: 10.1126/science.1146954.
- 308 2. Berghammer AJ, Klingler M, Wimmer E. A universal marker for transgenic insects.
309 Nature. 1999;402:370. doi: 10.1038/46463.
- 310 3. Lorenzen MD, Kimzey T, Shippy TD, Brown SJ, Denell RE, Beeman RW. *piggyBac*-
311 based insertional mutagenesis in *Tribolium castaneum* using donor/helper hybrids. Insect Mol
312 Biol. 2007;16(3):265-75. doi: 10.1111/j.1365-2583.2007.00727.x.
- 313 4. Gilles AF, Schinko JB, Averof M. Efficient CRISPR-mediated gene targeting and
314 transgene replacement in the beetle *Tribolium castaneum*. Development. 2015;142(16):2832-9.
- 315 5. Trauner J, Schinko J, Lorenzen MD, Shippy TD, Wimmer EA, Beeman RW, et al. Large-
316 scale insertional mutagenesis of a coleopteran stored grain pest, the red flour beetle *Tribolium*
317 *castaneum*, identifies embryonic lethal mutations and enhancer traps. BMC Biol. 2009;7(1):73.
318 doi: 10.1186/1741-7007-7-73.
- 319 6. Brown SJ, Mahaffey JP, Lorenzen MD, Denell RE, Mahaffey JW. Using RNAi to
320 investigate orthologous homeotic gene function during development of distantly related insects.
321 Evolution & Development. 1999;1(1):11-5. doi: 10.1046/j.1525-142x.1999.99013.x.
- 322 7. Bucher G, Scholten J, Klingler M. Parental RNAi in *Tribolium* (Coleoptera). Curr Biol.
323 12(3):R85-R6. doi: 10.1016/S0960-9822(02)00666-8.
- 324 8. Tomoyasu Y, Denell RE. Larval RNAi in *Tribolium* (Coleoptera) for analyzing adult
325 development. Dev Genes Evol. 2004;214(11):575-8. doi: 10.1007/s00427-004-0434-0.
- 326 9. Schmitt-Engel C, Schultheis D, Schwirz J, Ströhlein N, Troelenberg N, Majumdar U, et
327 al. The iBeetle large-scale RNAi screen reveals gene functions for insect development and
328 physiology. Nature Communications. 2015;6:7822. doi: 10.1038/ncomms8822
329 <https://www.nature.com/articles/ncomms8822-supplementary-information>.
- 330 10. Schinko JB, Weber M, Viktorinova I, Kiupakis A, Averof M, Klingler M, et al. Functionality
331 of the GAL4/UAS system in *Tribolium* requires the use of endogenous core promoters. BMC
332 Dev Biol. 2010;10(1):53. doi: 10.1186/1471-213x-10-53.
- 333 11. Dippel S, Kollmann M, Oberhofer G, Montino A, Knoll C, Krala M, et al. Morphological
334 and Transcriptomic Analysis of a Beetle Chemosensory System Reveals a Gnathal Olfactory
335 Center. BMC Biol. 2016;14(1):90. doi: 10.1186/s12915-016-0304-z.
- 336 12. Silver K, Jiang H, Fu J, Phillips TW, Beeman RW, Park Y. The *Tribolium castaneum* cell
337 line TcA: a new tool kit for cell biology. Sci Rep. 2014;4:6840. doi: 10.1038/srep06840
338 <https://www.nature.com/articles/srep06840-supplementary-information>.

- 339 13. Kim JH, Lee S-R, Li L-H, Park H-J, Park J-H, Lee KY, et al. High Cleavage Efficiency of
340 a 2A Peptide Derived from Porcine Teschovirus-1 in Human Cell Lines, Zebrafish and Mice.
341 PLOS ONE. 2011;6(4):e18556. doi: 10.1371/journal.pone.0018556.
- 342 14. Nie J, Mahato S, Zelhof AC. Imaging the Drosophila retina: zwitterionic buffers PIPES
343 and HEPES induce morphological artifacts in tissue fixation. BMC Dev Biol. 2015;15(1):10. doi:
344 10.1186/s12861-015-0056-y.
- 345 15. Naito Y, Hino K, Bono H, Ui-Tei K. CRISPRdirect: software for designing CRISPR/Cas
346 guide RNA with reduced off-target sites. Bioinformatics. 2015;31(7):1120-3. doi:
347 10.1093/bioinformatics/btu743.
- 348 16. Duffy JB. GAL4 system in drosophila: A fly geneticist's swiss army knife. Genesis.
349 2002;34(1-2):1-15. doi: 10.1002/gene.10150.
- 350 17. Ma J, Ptashne M. Deletion analysis of GAL4 defines two transcriptional activating
351 segments. Cell. 1987;48(5):847-53. doi: [https://doi.org/10.1016/0092-8674\(87\)90081-X](https://doi.org/10.1016/0092-8674(87)90081-X).
- 352 18. Viktorinová I, Wimmer EA. Comparative analysis of binary expression systems for
353 directed gene expression in transgenic insects. Insect Biochem Mol Biol. 2007;37(3):246-54.
354 doi: <https://doi.org/10.1016/j.ibmb.2006.11.010>.
- 355 19. Guimaraes JC, Zavolan M. Patterns of ribosomal protein expression specify normal and
356 malignant human cells. Genome Biology. 2016;17(1):236. doi: 10.1186/s13059-016-1104-z.
- 357 20. Sokoloff A, Faustini D. Dachs, a mutant in Tribolium with effects analogous to engrailed
358 in Drosophila. Journal of Heredity. 1987;78(1):2-7. doi: 10.1093/oxfordjournals.jhered.a110299.
- 359 21. Dawson PS. The "reindeer" mutation and a revision of linkage groups V and X in the
360 flour beetle, Tribolium castaneum. Canadian Journal of Genetics and Cytology. 1984;26(6):762-
361 4. doi: 10.1139/g84-120.
- 362 22. Brown E, Sokoloff A. LINKAGE STUDIES IN TRIBOLIUM CASTANEUM. XI. THE MAP
363 POSITION OF CHARCOAL, A PSEUDOALLELE OF BLACK. Canadian Journal of Genetics
364 and Cytology. 1978;20(1):139-45. doi: 10.1139/g78-014.
- 365 23. Groth AC, Fish M, Nusse R, Calos MP. Construction of Transgenic Drosophila by Using
366 the Site-Specific Integrase From Phage ϕ C31. Genetics. 2004;166(4):1775-82. doi:
367 10.1534/genetics.166.4.1775.
- 368 24. Goodman CL, Stanley D, Ringbauer JA, Beeman RW, Silver K, Park Y. A cell line
369 derived from the red flour beetle Tribolium castaneum (Coleoptera: Tenebrionidae). In Vitro Cell
370 Dev Biol Anim. 2012;48(7):426-33. doi: 10.1007/s11626-012-9524-x.
- 371 25. Bortoluzzi S, d'Alessi F, Romualdi C, Danieli GA. Differential expression of genes coding
372 for ribosomal proteins in different human tissues. Bioinformatics. 2001;17(12):1152-7. doi:
373 10.1093/bioinformatics/17.12.1152.
- 374 26. Thorrez L, Van Deun K, Tranchevent L-C, Van Lommel L, Engelen K, Marchal K, et al.
375 Using Ribosomal Protein Genes as Reference: A Tale of Caution. PLOS ONE.
376 2008;3(3):e1854. doi: 10.1371/journal.pone.0001854.

- 377 27. Sauert M, Temmel H, Moll I. Heterogeneity of the translational machinery: Variations on
378 a common theme. *Biochimie*. 2015;114:39-47. doi: <https://doi.org/10.1016/j.biochi.2014.12.011>.
- 379 28. Siebert KS, Lorenzen MD, Brown SJ, Park Y, Beeman RW. Tubulin superfamily genes in
380 *Tribolium castaneum* and the use of a Tubulin promoter to drive transgene expression. *Insect*
381 *Biochem Mol Biol*. 2008;38(8):749-55. doi: <https://doi.org/10.1016/j.ibmb.2008.04.007>.
- 382 29. Lorenzen MD, Brown SJ, Denell RE, Beeman RW. Transgene expression from the
383 *Tribolium castaneum* Polyubiquitin promoter. *Insect Mol Biol*. 2002;11(5):399-407. doi:
384 10.1046/j.1365-2583.2002.00349.x.
- 385 30. Osanai-Futahashi M, Tatematsu K-i, Yamamoto K, Narukawa J, Uchino K, Kayukawa T,
386 et al. Identification of the Bombyx Red Egg Gene Reveals Involvement of a Novel Transporter
387 Family Gene in Late Steps of the Insect Ommochrome Biosynthesis Pathway. *J Biol Chem*.
388 2012;287(21):17706-14. doi: 10.1074/jbc.M1111.321331.
- 389 31. Broehan G, Kroeger T, Lorenzen M, Merzendorfer H. Functional analysis of the ATP-
390 binding cassette (ABC) transporter gene family of *Tribolium castaneum*. *BMC Genomics*.
391 2013;14(1):6. doi: 10.1186/1471-2164-14-6.
- 392 32. Grubbs N, Haas S, Beeman RW, Lorenzen MD. The ABCs of Eye Color in *Tribolium*
393 *castaneum*: Orthologs of the *Drosophila* white, scarlet, and brown Genes. *Genetics*.
394 2015;199(3):749-59. doi: 10.1534/genetics.114.173971. PubMed PMID: PMC4349069.
- 395 33. Arakane Y, Lomakin J, Beeman RW, Muthukrishnan S, Gehrke SH, Kanost MR, et al.
396 Molecular and Functional Analyses of Amino Acid Decarboxylases Involved in Cuticle Tanning
397 in *Tribolium castaneum*. *J Biol Chem*. 2009;284(24):16584-94. doi: 10.1074/jbc.M901629200.
398